Presented at the First Canadian Symposium on Numerical Applications
in Mining and Geomechanics, March 27-30, 1993, Montreal, Canada.

MODELLING DISCONTINUOUS ROCKMASSES IN THREE DIMENSIONS USING MAP3D

Terry D. Wiles
Mine Modelling Ltd.

D. Nicholls
Inco Manitoba Ltd.

ABSTRACT

In this paper, several examples of the use of MAP3D (three-dimensional stress analysis program), to simulate discontinuous rockmass response are presented. This simulation capability has been achieved by incorporation of displacement discontinuities into the indirect boundary element procedure used in MAP3D. Fault slip and crack opening can both be accommodated.

To build the mining geometries, one need only specify the features of interest, i.e. the mining blocks and the faults. The intersection between these entities, detection of overlap areas and discretization into boundary elements, is automatically conducted by MAP3D as part of the analysis.

Application to real mining problems illustrate that the incorporation of fault slip can have an overwhelming influence on the rockmass response. Stresses and displacements are redistributed, thus enhancing stability at some locations, but increasing stress concentrations at others.

INTRODUCTION

Linear elastic, three-dimensional numerical modelling is now conducted on a routine basis at many mining camps. This is a result of the recognition of the importance of three-dimensional effects, recent progress in ease of use of 3-D numerical models, and the enormous increase of the computation power of affordable personal computers.

The influence of discontinuities such as faults and joints is normally not considered, even though both finite element (Goodman fault element, Goodman, 1976) and distinct element (UDEC and 3DEC, Cundall, 1971) codes with this capability have been available for some time. While the importance of fault slip is well understood, simulation of discontinuous rockmasses is at present undertaken only for special modelling projects normally involving consultants or expert research staff. This situation exists because of the difficulty in setting up and using these models, and the long run times required for such simulations.

Although the displacement discontinuity technique (NFOLD, MINTAB, DZTAB, EXAMINETAB, see Starfield and Fairhurst, 1968) has been used extensively for the simulation of tabular mining problems, very few models have incorporated this facility into a three-dimensional boundary element analysis program. MAP3D (Wiles, 1993) does have this capability. Combined with the ability to automatically build intersections between bisecting faults and excavations, this overcomes the complication of setting up and using these models, while maintaining ease of use and short run times.

DISPLACEMENT DISCONTINUITIES IN THE BOUNDARY ELEMENT METHOD

The MAP3D model formulation is based on the indirect boundary element method. For the case of a homogeneous, elastic medium, an indirect boundary element procedure known as the fictitious force method (Banerjee and Butterfield, 1981) can be stated as follows

$$\sigma^s = \mathbf{T} \cdot \sigma^f + \mathbf{C} \cdot \mathbf{P} \qquad (1)$$

where σ^s represents a vector of normal and shear stresses acting on the boundary elements at the surfaces of the excavations, σ^f represents the far field stress state, $\mathbf{T}$ represents the stress transformation matrix from the axes of the far field stress state to the axes at each boundary element, $\mathbf{P}$ represents the normal and shear (fictitious) forces applied at each boundary element, and $\mathbf{C}$ represents a matrix of influence coefficients relating the applied normal and shear forces $\mathbf{P}$ to the stress change at each boundary element.

In order to incorporate displacement discontinuities into the solution process, one need only superimpose their effects on the existing geometry. This requires that the influence of each displacement discontinuity (Wiles and Curran, 1982) be determined, at every other boundary element, thus adding additional rows and columns to the $\mathbf{C}$ matrix. The additional unknowns added to the vector $\mathbf{P}$ represent the amount of ride (fault slip) and closure (or crack opening) on the displacement discontinuity surfaces.

In a normal boundary element analysis procedure, the stresses σ^s and σ^f are specified, the matrices $\mathbf{T}$ and $\mathbf{C}$ are calculated from the geometry, and then the unknown vector $\mathbf{P}$ is solved for using the above equations. To incorporate the influence of the displacement discontinuities, it is

necessary to evaluate the normal and shear stresses acting on each displacement discontinuity surface during the solution process. If the shear stress is less than the shear strength (determined for example using a Mohr-Coulomb failure criterion), then the amount of fault slip is zero. Alternatively, if the shear stress exceeds the shear strength, then the shear stress is set equal to the strength

$$\tau = S_0 + \sigma_n \cdot \tan\phi \qquad (2)$$

where σ_n represents the normal stress, and S_0 and ϕ represent respectively the cohesion and friction angle. The amount of fault slip is solved for as part of the matrix solution along with the other components of vector P.

More complex fault response can be easily incorporated by using additional expressions relating the normal and shear stresses to the closure and ride. This can include the simulation of gouge material, non-linear normal stiffness, dilation, peak and residual strengths etc. While these effects are well known (Goodman, 1976, Bandis et al, 1983, Saeb and Amadei, 1992), they are also very difficult to accurately quantify.

SUPERIMPOSING FAULTS ON EXCAVATION GEOMETRIES

In the mining example illustrated in figure 1, an inclined fault intersects a simple rectangular shaped stope. This example is presented to illustrate the far reaching influence that the presence of a fault can have on the rockmass response around an excavation.

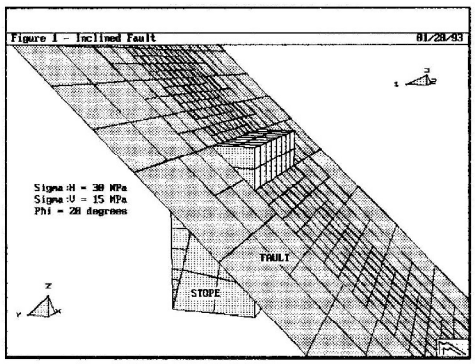

To build this geometry in MAP3D, one need only specify two features, the stope and the fault. The intersection between these entities, detection of overlap areas and discretization into boundary elements, is automatically conducted by MAP3D as part of the analysis. This figure illustrates the final boundary element mesh, ready for analysis.

In this problem, the far field stress state has been specified as 30MPa in both horizontal directions, and 15MPa in the vertical direction. The elastic properties of the host rockmass are Young's modulus of 60GPa and Poisson's ratio of 0.25. The stope is 2m wide, 4m high and 4m long (along strike). The fault dips at 45° and strikes parallel to the stope. The fault has a friction angle of 20° with no cohesion. At the far field

stress state, the fault has a strength of 8.2MPa and an active shear stress of 7.5MPa, giving a safety factor of 1.1, a stable condition.

In the adjacent figures, analysis results are presented on a transverse section taken at the mid-point of the stope. Owing to slip on the fault, it can be observed that (figure 2) the major principal stress is distributed non-uniformly around the stope. The presence of the fault has significantly reduced the stress concentration directly over the top of the stope, and redistributed the stresses adjacent to the fault slip area.

Figure 3 illustrates that the minor principal stresses are even more intensely redistributed, showing a reduction in the stress concentration over the upper right hand corner of the stope, and the development of some tensile stresses.

The displacements (figure 4) show reduced closure of the stope in the area above and to the right of the fault.

During the analysis, the fault slips a maximum of 0.14mm at the side of the stope. This occurs over a length of almost 2m. In the area directly above the stope, the fault slips a maximum of 0.6mm. This slip occurs over a length of more

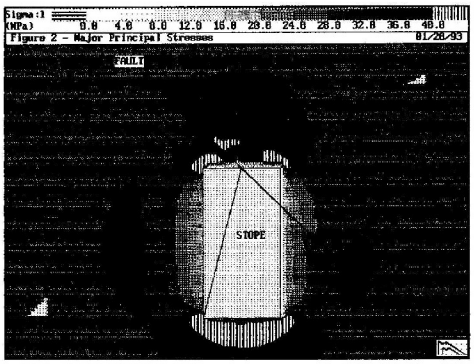

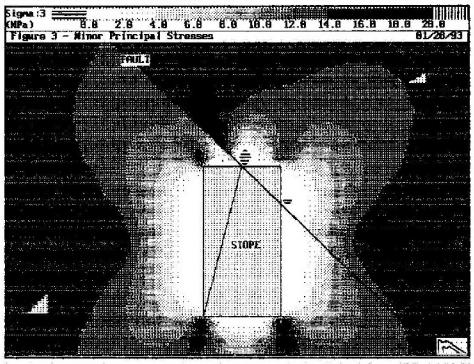

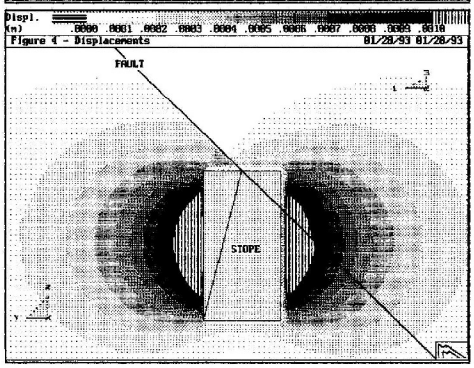

than 5m. As the stope is only 2m wide, this represents a relatively far reaching influence.

HANGINGWALL AND FOOTWALL FAULTS PASSING NEAR MINING BLOCKS

At the INCO Thompson Birchtree Mine, there are well defined fault zones in both the hangingwall and footwall of the orebody. The location of these relative to the mining blocks is illustrated in figure 5 which shows a three-dimensional perspective view looking down in a south-east direction.

The rockmass at this mine is well jointed and very weak. A far field stress state of 38MPa acting in the hangingwall- footwall direction (east-west), 25MPa acting along the strike of the orebody, and 16MPa vertical, has been used. The Young's modulus of the rockmass is 13.5GPa, with a Poisson's ratio of 0.25. Both faults have been assigned a Young's modulus of 5GPa with a gouge thickness of 1m, and a friction angle of 20° with no cohesion.

Figures 6 and 7 show the major principal stresses around the 21800 block in Birchtree Mine respectively without and with the faults. The view shows a transverse section, positioned such that the observer is looking directly along the strike of

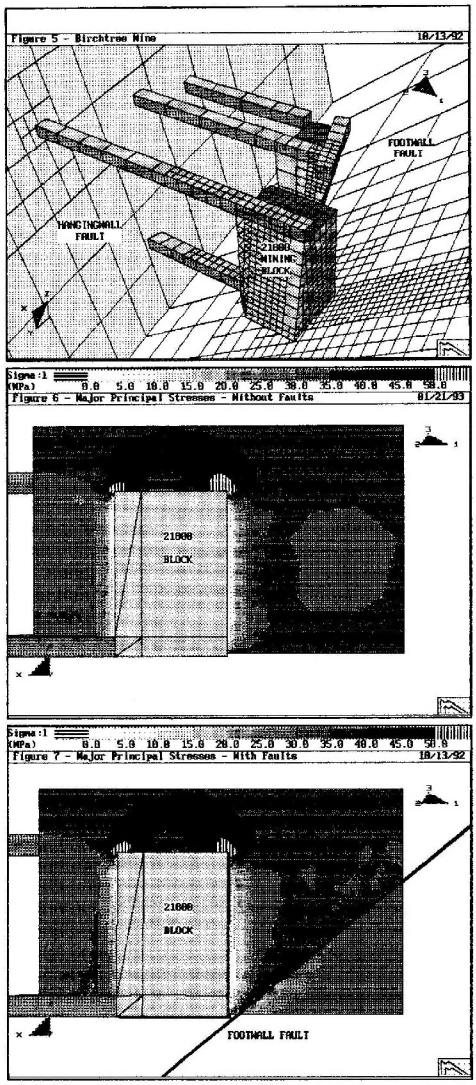

the footwall fault. In these figures it can be observed that the presence of the faults does not significantly influence the magnitude of the major principal stresses, except in the immediate vicinity of the fault.

However, the minor principal stresses (figures 8 and 9) are significantly reduced both over the back of the mining block, and at the lower portion of the footwall side of the block. In the zone for the first 5m above the back of the block, the confinement goes from 2 to 4MPa without the faults, to less than 2MPa, with both faults. Along the lower footwall side of the mining block, the tension zone more than doubles in size, from 1.6m to nearly 4m thickness.

The displacements are illustrated in figures 10 and 11. These figures show that due to the presence of the faults, the total closure across the mining blocks increases from 0.077m to 0.1m (30% increase). The footwall fault shears a maximum of 0.06m near the lower footwall side of the mining block.

Although in this case the stress changes predicted by the model appear to be insignificant between the case with and without the discontinuity, in a rockmass as weak and unstable as this, small changes can cause real problems. In this orebody, instability is usually

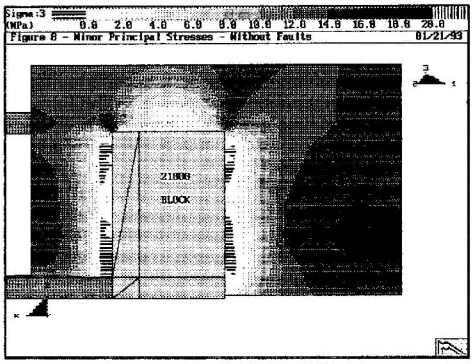

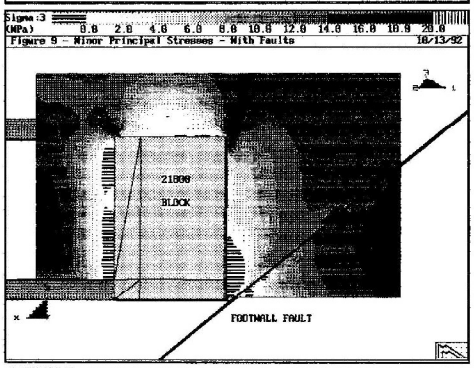

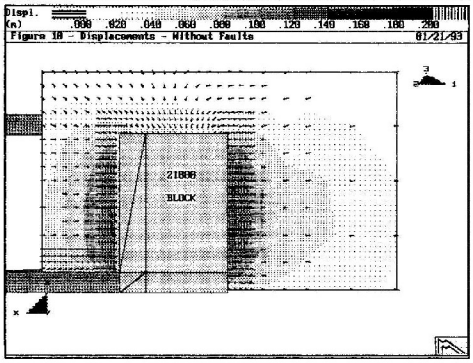

associated with low confinement zones. The zone of low stress over the back of the mining block represents a large volume of material.

This is further emphasized by considering the minor principal stresses on a longitudinal section taken through the same mining block. Figures 12 and 13 show that the confinement in the pillar between the two mining blocks has increased due to the presence of the faults. The increase in the confinement in this pillar is sufficient to bring the safety factor from below one, to well above one through most of the pillar.

The tension zones have also moved. Note the formation of a tension zone adjacent to the access drift at the top of the 21800 block. Also, the tension zone at the upper right side (north) of this block has moved to the bottom of this face.

We believe at this time that the footwall discontinuity is stable and have not seen, by visual observation, any movement along the exposed sections of this fault. Strain measuring devices will be installed across the fault to determine if there is movement that cannot be detected visually. The results from these will be used to further calibrate the model.

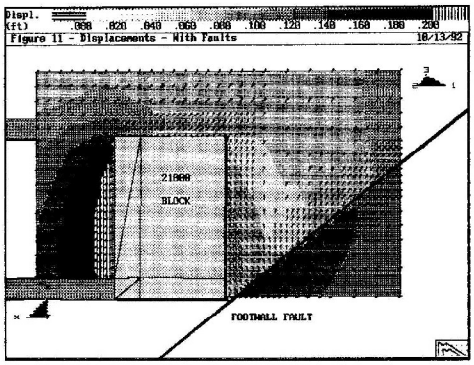

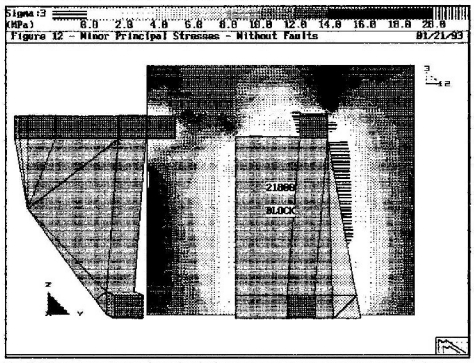

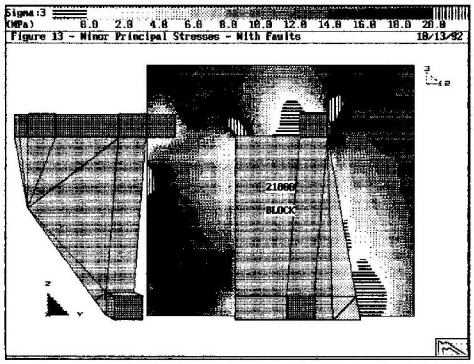

HANGINGWALL PILLAR FORMED BY A WEAK FAULT

This final example illustrates a near surface mining problem where a weak fault is located 3m into the hangingwall of the mine. The shape of the stope has been simplified to a rudimentary rectangular shape with dimensions of 30m along strike, 30m high and 12m thick, as shown in figure 14.

For this analysis, the far field stresses have been assumed to vary linearly with depth giving, at the mid-height of the mining block (35m depth), a maximum horizontal far field stress of 14MPa oriented parallel to the strike of the fault. The other horizontal stress and the vertical stress are equal to 3.2MPa. The rockmass is assumed to have a Young's modulus of 25GPa and a Poisson's ratio of 0.25. The fault has been given 1m of gouge with a modulus 5GPa, and a friction angle of 9°.

Simple calculations illustrate that owing to the low frictional strength of the fault, it is necessary that the maximum horizontal far field stress be oriented less than 3° from the strike of the fault or else the fault will be over-stressed and unstable.

The predicted major and minor principal stresses are illustrated on a transverse section taken at the mid-

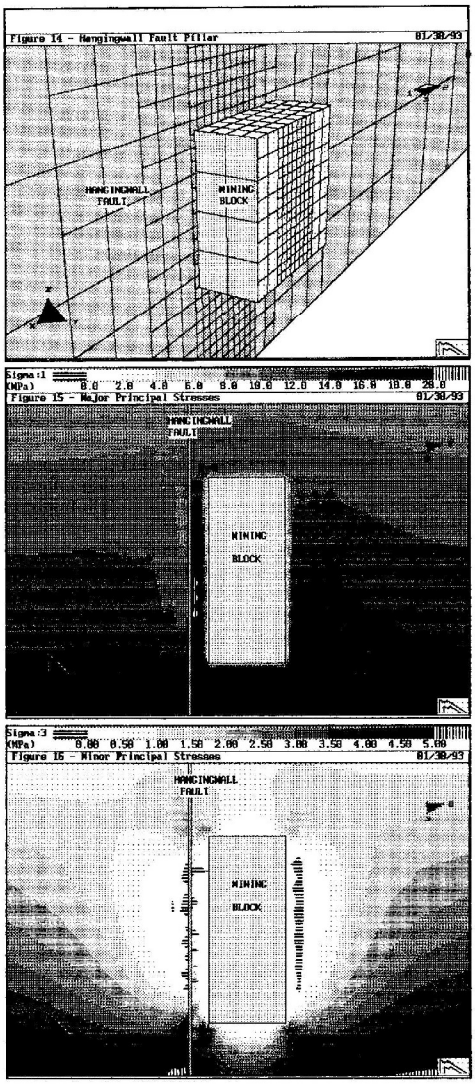

point of the mining block. In figure 15, it can be observed that the major principal stress is concentrated in the ground between the fault and the hangingwall side of the mining block. At this same location, the minor principal stress is zero or tensile (figure 16). Under these conditions it is unlikely that the ground will remain stable.

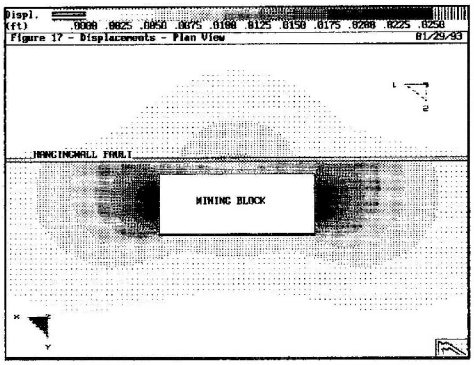

It appears that the fault causes the 2m of ground between the fault and hangingwall side of the mining block to act as a pillar. This is because the normal arching of stresses around the hangingwall side of the mining block are partially cut-off by the fault, and directed through the pillar instead of out into the hangingwall.

In figure 17, the rockmass displacements are shown on a plan taken at the mid-height of the mining block. It is clearly illustrated here that the fault slips for at least one strike length of the mining block on either side of the stope. On a mining scale this would represent a very large distance.

SUMMARY AND CONCLUSIONS

The examples presented in this paper demonstrate that discontinuous rockmasses can be modelled in 3-dimensions using the MAP3D analysis program.

Three different mining geometries have been presented. Each of these tests a different mode of fault slip. In all three cases, slip on the fault has resulted in significant redistribution of stresses. The first example illustrates a fault intersecting a stope. Fault slip occurred as far as 2.5 times the stope width away.

The second example illustrates a mining case where the footwall fault passes just below the mining block. Slip of 0.06m on this fault results in the movement of tension zones to different locations around the mining block. The confinement in the pillar between the mining blocks is elevated thus increasing its stability.

In the third example, a weak fault in the hangingwall of the mine results in a loss of arching into the hangingwall rocks, thus loading up the

pillar formed by the hangingwall side of the mining block and the fault. This coupled by the loss of confinement in this pillar would likely lead to instability in this pillar. Slip of nearly 0.003m occurs adjacent to the mining block. The fault moves at a maximum distance of one strike length away from the mining block. For a large mine this could represent a very large distance.

Since the discontinuities are incorporated into the boundary element analysis procedure, only the boundaries are discretized, thus complex problems can be simulated with relative ease. The advantages of the boundary element method, over domain methods such as the finite element or finite difference techniques, is maintained.

Model construction is very easy since MAP3D automatically builds intersections between mining blocks and faults. The detection of overlapping areas and discretization into boundary elements, is automatically conducted by MAP3D as part of the analysis.

With this capability, users can now readily consider the effect of fault slip on their mine designs. The authors feel that this is a very important step, as the accuracy and reliability of mine designs will be enhanced.

REFERENCES

Bandis, S., A. Lumsden and N. Barton, 1983, Fundamentals of Rock Joint Deformation, Int. J. Rock Mech. Min. & Geo. Abstr., V. 20, pp. 249-268.

Banerjee, P.K. and R. Butterfield, 1981, Boundary element analysis methods in engineering science, McGraw-Hill Book Comp Limited, New York.

Cundall, P.A., 1971, A Computer Model for Simulating Progressive, Large Scale Movements in Blocky Rock Systems, ISRM Symp., Nancy, France.

Goodman, R.E., 1976, Methods in Geological Engineering in Discontinuous Rocks, West Publishing Comp., New York.

Saeb, S. and B. Amadei, 1992, Modelling Rock Joints under Shear and Normal Loading, Int. J. Rock Mech. Min. & Geo. Abstr., V. 29, N. 3, pp. 267-278.

Starfield, A.M. and C. Fairhurst, 1968, How High-Speed Computers Advance Design of Practical Mine Pillar Systems, Energy Min. J., pp. 78-84.

Wiles T.D., and J.H. Curran, 1982, The use of 3-D Displacement Discontinuity Elements for Modelling, Proc. 4th Int. Conf. Num. Methods in Geomech., Edmonton, Alberta, pp. 103-112.

Wiles T.D., 1993, MAP3D user manual, Mine Modelling Limited, Copper Cliff, Ontario, Canada.